Title

A computationally efficient exact pseudopotential method. II. Application to the molecular pseudopotential of an excess electron interacting with tetrahydrofuran (THF)

Journal

Journal of Chemical Physics, 125(7)

ISSN

0021-9606

Authors

Smallwood, C J
Mejia, C N
Glover, W J
et al.

Publication Date

2006-08-01

Peer reviewed

A computationally efficient exact pseudopotential method. II. Application to the molecular pseudopotential of an excess electron interacting with tetrahydrofuran (THF)

C. Jay Smallwood, Cesar N. Mejia, William J. Glover,
Ross E. Larsen, and Benjamin J. Schwartz[a)]
Department of Chemistry and Biochemistry, University of California, Los Angeles, Los Angeles, California 90095-1569

(Received 8 August 2005; accepted 7 June 2006; published online 16 August 2006)

In the preceding paper, we presented an analytic reformulation of the Phillips-Kleinman (PK) pseudopotential theory. In the PK theory, the number of explicitly treated electronic degrees of freedom in a multielectron problem is reduced by forcing the wave functions of the few electrons of interest (the valence electrons) to be orthogonal to those of the remaining electrons (the core electrons); this results in a new Schrödinger equation for the valence electrons in which the effects of the core electrons are treated implicitly via an extra term known as the pseudopotential. Although this pseudopotential must be evaluated iteratively, our reformulation of the theory allows the exact pseudopotential to be found without ever having to evaluate the potential energy operator, providing enormous computational savings. In this paper, we present a detailed computational procedure for implementing our reformulation of the PK theory, and we illustrate our procedure on the largest system for which an exact pseudopotential has been calculated, that of an excess electron interacting with a tetrahyrdrofuran (THF) molecule. We discuss the numerical stability of several approaches to the iterative solution for the pseudopotential, and find that once the core wave functions are available, the full e^--THF pseudopotential can be calculated in less than 3 s on a relatively modest single processor. We also comment on how the choice of basis set affects the calculated pseudopotential, and provide a prescription for correcting unphysical behavior that arises at long distances if a localized Gaussian basis set is used. Finally, we discuss the effective e^--THF potential in detail, and present a multisite analytic fit of the potential that is suitable for use in molecular simulation. © *2006 American Institute of Physics*. [DOI: 10.1063/1.2218835]

I. INTRODUCTION

There are a very limited number of systems of interest in chemistry and condensed-matter physics that have only a few electrons; however, few-electron systems are currently the boundary for exact quantum mechanical calculations. As such, it is imperative to find approximations to the many-electron problem that provide for accurate wave functions and energies but avoid explicit computation of most of the electrons. The standard approach to reduce the number of electrons is to first separate the many-electron system into core and valence electrons. This separation is based on the fact that core electrons are typically static during chemical processes so that by treating the core-valence and core-core electron interactions approximately, an exact calculation can be done for the small number of valence electrons while still retaining the important physics of the system. One of the most common approximations is to implicitly include the effects of the core electrons on the valence electrons by adding a new potential, known as a pseudopotential, to the valence electron Hamiltonian. Pseudopotentials have been used in a wide variety of fields ranging from solid-state electronic structure calculations[1] to mixed quantum/classical molecular dynamics.[2–6]

Although pseudopotentials are often developed empirically,[1,7] it is possible to rigorously derive a pseudopotential based on quantum mechanical theory; such a formalism was first developed by Phillips and Kleinman[8] (PK) and has been extended by others (see, e.g., Ref. 7 and references therein). The PK theory provides a quantum mechanical solution for the valence electrons by solving a modified eigenvalue equation that includes a nonlocal pseudopotential term. Historically, however, the use of the PK theory has been plagued by two main implementation issues. First, the theory requires accurate solutions for the core electron wave functions. Second, even if the core electron wave functions are available, solving for the valence electrons in the modified eigenequation is computationally expensive because the nonlocal pseudopotential necessitates an iterative solution of the PK equation. Therefore, several approximate schemes have been used in lieu of calculating the exact pseudopotential, including the use of approximate Hamiltonians[9] and the use of model wave functions for the core electrons.[10,11] The use of model wave functions works particularly well for systems where there is a great deal of intuition about the shape of the core wave functions, such as with atomic orbitals, but in molecular systems where the core wave functions are more complex, this type of approximation rapidly loses accuracy. Thus, for molecular systems, accurate results require a direct

[a)]Electronic mail: schwartz@chem.ucla.edu

solution of the PK equation; unfortunately, complex molecular systems are the very ones for which direct application of the PK formalism is the least computationally feasible.

In the preceding paper,[12] we presented an analytically exact reformulation of the PK pseudopotential theory. The principal advantage of our reformulation is that it is highly computationally efficient. Our method avoids the need to calculate the potential energy operator and its two-electron integrals during the self-consistent solution of the PK eigenequation, thus eliminating what is the rate-limiting step for solving any many-electron problem. In this paper, we illustrate the implementation of our formalism for a complex molecular pseudopotential; in particular, we compute the exact PK pseudopotential for a single excess electron interacting with a (closed shell) tetrahydrofuran (THF) molecule. We chose this system for two main reasons. First, this system is an excellent testbed for demonstrating the advantages of our method. There is little intuition by which to approximate the THF core molecular wave functions, and to the best of our knowledge, there has been no molecule as large as THF for which the exact pseudopotential has been calculated. In fact, we will demonstrate below that with our new formalism, calculation of the THF-electron pseudopotential is computationally trivial, opening the way to molecules of much greater complexity. Second, our group has a long-standing interest in experiments and nonadiabatic mixed quantum/classical molecular dynamics simulations of both solvated electrons[2,13,14] and sodium anions[3,15–19] in liquid THF. In the past,[2] we have specified how the quantum mechanical electron interacts with the classical THF molecules in simulations by using an empirical pseudopotential based on physical ideas presented by Liu and Berne.[20] In future work, we will compare mixed quantum/classical electron-THF simulations using the exact pseudopotential presented here to those using the empirical pseudopotential presented in our previous work; the results should allow us to learn a great deal about how accurate a pseudopotential must be to obtain reliable results in mixed quantum/classical molecular simulations.

The rest of this paper is organized as follows. In Sec. II, we summarize our formalism in the context of providing a computationally efficient procedure for the calculation of exact pseudopotentials. We then discuss the numerical implementation of our procedure for the specific case of an excess electron interacting with a THF molecule. Next, we address issues concerning how the calculated pseudopotential depends on the choice of basis set, and we present the full calculated exact e^--THF effective potential in detail. In Sec. III we describe how we fit the resulting pseudopotential to a set of analytic functions for use in molecular simulation and comment on the accuracy of our fit. We conclude in Sec. IV.

II. CALCULATION OF THE EXACT ELECTRON-THF PSEUDOPOTENTIAL

A. Review of the pseudopotential formalism

Since we will be applying a new formalism for the calculation of exact pseudopotentials, we begin our discussion by giving a brief description of the underlying theory; a full description of the theory can be found in the preceding paper, Ref. 12. The goal of pseudopotential theory is to reduce the number of explicitly treated electronic degrees of freedom (in our case, to one valence electron) by implicitly including the effects of the lower-lying core electrons (which we define as those electrons that remain approximately static during the physical process of interest) as an additional potential term to the Hamiltonian. As discussed in Ref. 12, constructing the pseudopotential is equivalent to writing the valence electron wave function in a basis that has been made orthogonal to the core-electron wave functions. The core and valence electronic wave functions are the eigenvectors of the Hamiltonian, $\hat{H}=\hat{T}+\hat{U}$. The core-electron eigenstates are given by

$$\hat{H}|\psi_i\rangle = \epsilon_i|\psi_i\rangle \quad (i=1,\text{ncore}), \tag{1}$$

where ncore is the total number of core electrons and the valence electron wave function is given by

$$\hat{H}|\psi_v\rangle = \epsilon|\psi_v\rangle. \tag{2}$$

If the valence electron is represented in a basis for which each basis function has been *a priori* orthogonalized to every core-electron wave function, then Eq. (2) becomes[8]

$$\hat{H}|\phi\rangle + \sum_{i=1}^{\text{ncore}} |\psi_i\rangle\langle\psi_i|\epsilon - \hat{H}|\phi\rangle \equiv [\hat{H}+\hat{V}_p]|\phi\rangle = \epsilon|\phi\rangle. \tag{3}$$

This is the Phillips-Kleinman pseudopotential equation. It has the same structure as Eq. (2) except that there is an additional potential term, the pseudopotential $\hat{V}_p$. The ground-state solution to this effective Hamiltonian, $\hat{H}+\hat{V}_p$, is called the pseudo-orbital, $|\phi\rangle$, and has an energy identical to that of the valence electron. The relationship between the pseudo-orbital and the valence electron arises from the preorthogonalization of the basis set,

$$|\psi_v\rangle = |\phi\rangle - \sum_{i=1}^{\text{ncore}} |\psi_i\rangle\langle\psi_i|\phi\rangle. \tag{4}$$

Thus, the valence electron solutions to the PK pseudopotential equation are guaranteed to be orthogonal to the core electrons. Moreover, since $|\phi\rangle \rightarrow |\psi_v\rangle$ outside the core electron region, solving Eq. (3) for the pseudo-orbital suffices to solve the problem away from the core.

The pseudo-orbital solution to Eq. (3), however, is not unique;[21] thus, we can impose an additional constraint that does not affect the orthogonality between the valence and core electron wave functions. By choosing a constraint in which the expectation value of the pseudo-orbital is extremized with respect to an arbitrary operator $\hat{F}$, we can find a unique solution for the pseudo-orbital by solving,

$$\hat{H}|\phi\rangle + \sum_{i=1}^{\text{ncore}} |\psi_i\rangle\langle\psi_i|\epsilon - \hat{H} + \hat{F} - \bar{F}|\phi\rangle = \epsilon|\phi\rangle, \tag{5}$$

where $\bar{F}=\langle\phi|\hat{F}|\phi\rangle/\langle\phi|\phi\rangle$ is the expectation value of $\hat{F}$ for the pseudo-orbital $|\phi\rangle$. As discussed in the Introduction, Eq. (5) is computationally expensive to solve, which has limited its use and forced researchers to work with various approximate schemes. In Ref. 12, however, we showed that instead

of solving Eq. (5), the same unique pseudo-orbital $|\phi\rangle$ can be calculated by solving

$$|\phi\rangle = |\psi_v\rangle + \sum_{i=1}^{\text{ncore}} \frac{\langle\psi_i|\hat{F}|\phi\rangle}{\bar{F}}|\psi_i\rangle. \tag{6}$$

If we choose to minimize the expectation value of the kinetic-energy operator, so that $\hat{F}=\hat{T}$, the self-consistent solution for the pseudo-orbital via Eq. (6) entirely avoids the computation of the potential energy operator. Since the potential energy term involves the calculation of two-electron integrals, the evaluation of the potential energy is always the slow step in multielectron calculations. In this paper, we will use kinetic-energy minimization to calculate the excess e^--THF pseudopotential since our formulation with this choice removes the main computational bottleneck.

Once the unique pseudo-orbital has been calculated via Eq. (6), it is straightforward to calculate the pseudopotential. For molecular simulations and other applications, however, what is most often needed is the total effective potential U_{eff}, which includes the potential from the original Hamiltonian as well as the additional repulsive pseudopotential $\hat{V}_p$, that arises from preorthogonalization. Unfortunately, the pseudopotential arising from the solution to Eq. (6) is nonlocal, making its on-the-fly evaluation impractical for use in simulations. However, the fact that $|\phi\rangle$ is the ground-state solution to Eq. (5) means that it can be made nodeless,[12] allowing the total effective potential from the kinetic-energy-minimized pseudo-orbital determined from Eq. (6) to be localized by

$$U_{\text{eff}}^{\text{local}}(\mathbf{r}) = \frac{\langle\mathbf{r}|(\epsilon-\hat{T})|\phi\rangle}{\langle\mathbf{r}|\phi\rangle}. \tag{7}$$

So, if we choose to minimize the kinetic energy, our formalism allows us to avoid calculating the potential energy operator entirely after the initial step of finding the core and valence electron wave functions.[12] With all the pieces in place, we apply this formalism to calculate the effective potential for a complex molecular system, namely, an excess electron interacting with a THF molecule.

B. Computational details in solving for the THF-e^- pseudopotential

The first step in calculating the local effective potential for an excess electron interacting with a THF molecule was to find the core and valence electron wave functions, Eqs. (1) and (2), of THF. In line with previous work on molecular pseudopotentials,[9,22,23] we solved for the molecular orbitals (MOs) of THF using closed-shell Hartree-Fock theory[24] within the frozen-core approximation[25] (i.e., we assumed that the closed-shell core electrons are not altered by the presence of the excess electron) using the GAUSSIAN 98 program.[26] The basis set used, 6-31++G(AUG), consisted of an atom-centered 6-31++G Pople basis set augmented with an additional $8^3=512$ *s*-type Gaussian primitives that were evenly distributed over a cubic grid of side $150a_0$, where a_0 is the Bohr radius; the total number of contractions was 601. We will discuss the details of this particular augmented basis set further below in Sec. II C. For now, we note that a similar augmented basis set was used successfully by Turi *et al.* in determining the pseudopotential of an excess electron interacting with water.[22]

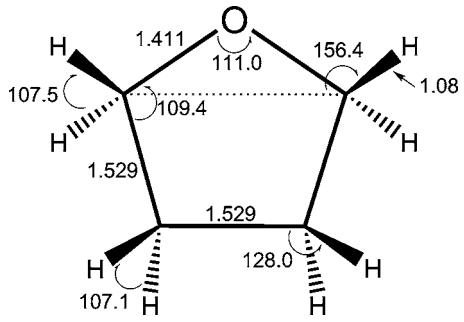

FIG. 1. Hydrogen-optimized planar THF structure used in this work. The bond distances are given in angstroms (Å) and angles are in degrees. When projected onto the molecular plane, the alpha hydrogens make a 156.4° angle with respect to the dotted line connecting the alpha carbons and the beta hydrogens form a 128.0° angle with respect to the analogous line connecting the beta carbons.

Since our interest in developing the electron-THF pseudopotential is to employ it in mixed quantum/classical simulations of liquid THF, we chose the geometry of the THF molecule to match that of the classical THF model developed by Jorgenson and co-workers;[27] the geometry of this model of THF is shown in Fig. 1. Thus, even though the fully-optimized structure of THF is bent (and at finite temperature undergoes pseudorotation), we calculated the pseudopotential for a THF molecule constrained so that all four C atoms and the O atom are co-planar. The use of planar THF model for simulations of the liquid has been justified by Chandrasekar and Jorgenson, who found that both planar and pseudorotating bent models of THF produced identical solvent packing.[27] Moreover, and perhaps more importantly, approximating the THF molecule as planar avoids the difficulty of having to calculate a different pseudopotential for every possible bent geometry. Since we plan to employ Chandrasekar and Jorgenson's planar model of THF for mixed quantum/classical simulations, we calculated the electron-THF pseudopotential for this geometry to ensure internal consistency in our upcoming simulations and to facilitate comparisons with our previous simulations of the THF-solvated electron that also used this model for liquid THF.[2] The THF geometry we used to calculate our pseudopotential does, however, include one important structural difference from Chandrasekar and Jorgenson's planar model. Their model employed united atoms for the methylene groups to avoid explicit inclusion of the hydrogen atoms,[27] but as we demonstrate below in Sec. II D, explicit inclusion of the hydrogen atoms is essential to correctly reproduce the exact pseudopotential. Thus, even though it will require calculating the positions of hydrogen atoms that are not present in the classical THF simulation model, we must include the hydrogen atoms in the calculation of the pseudopotential in our upcoming simulations. To determine the positions of the hydrogen atoms, we calculated the energy-minimized electronic structure of the THF molecule by first constraining the heavy atoms of the backbone to match the geometry of the

planar Chandrasekar-Jorgensen model and we then allowed the positions of the hydrogen atoms to optimize. The 20 occupied core MOs and the lowest unoccupied molecular orbital (LUMO) (which is the valence electron within the static-exchange approximation) of this hydrogen-optimized planar structure are what was used to calculate the pseudopotential.

For THF, we found that the direct iterative solution of Eq. (6) to find the pseudo-orbital is numerically unstable. Instead, as in Ref. 12, we found that we could achieve a stable numerical solution for the pseudo-orbital using an iterative matrix-inversion scheme to solve the rearranged equation,

$$|\phi\rangle = \left[I - \frac{\hat{\Omega}\hat{T}}{\hat{T}} \right]^{-1} |\psi_v\rangle \equiv \hat{M}^{-1}|\psi_v\rangle, \tag{8}$$

where $\hat{T}$ is the kinetic energy operator and $\hat{\Omega}=\Sigma_{i=1}^{\text{ncore}}|\psi_i\rangle\langle\psi_i|$ is the projection operator onto the occupied core MOs.[12] To iteratively solve Eq. (8), we expanded the matrix in terms of our contracted Gaussian basis set, solved the linear matrix equation, $\hat{M}|\phi\rangle=|\psi_v\rangle$ using LAPACK routines,[28] and used the resulting coefficients for $|\phi\rangle$ to form the matrix for the next iteration. For our convergence criterion, we required that the values of the basis set coefficients for $|\phi\rangle$ on successive iterations did not change within machine precision. For our choice of basis set, if we used a wave function comprised 90% of the THF LUMO as a starting guess, it took less than 3 s for the solution of Eq. (8) to converge on a single AMD64 2.2 GHz serial processor. In addition to the rapid convergence, the solution to Eq. (8) is robust. For example, although it is typical for the LUMO to comprise ~90% of the pseudo-orbital,[7,8,21] as we have found to be the case for THF, wildly unphysical starting guesses (e.g., assuming that the pseudo-orbital was composed 90% of lowest energy symmetry allowed core orbital) still converged within four iterations. Having obtained the pseudo-orbital coefficients, the spatially localized effective potential was calculated directly using Eq. (7), as described in more detail below in Sec. II D.

C. Choice of basis set

Equation (6) makes it is clear that the quality of the pseudo-orbital will depend on the quality of the core and valence orbitals used to generate it. Thus, it is imperative to select a basis set that correctly captures the electron distribution of both the core and valence orbitals. For THF, the core orbitals, which correspond to the 20 occupied MOs, are tightly bound to the molecular frame of THF. Indeed, during our initial basis set exploration, the core orbitals proved to be quite insensitive to the choice of basis beyond a set of moderate size. In other words, the energy and structure of the core orbitals changed little when going from a moderate-sized basis set, such as 6-31++G (89 contractions), to a large basis set, such as aug-cc-pVTZ (414 contractions). Because THF is a neutral closed shell molecule, however, the valence orbital (LUMO) is expected to be rather large and diffuse. In fact, under the frozen-core approximation, an excess electron in the vicinity of THF is predominantly dipole bound; indeed, the 1.75 D dipole moment of THF (Ref. 29) exceeds the critical value needed to create a dipole-bound anion.[30] Therefore, to calculate an accurate LUMO, it is critical that we choose a basis set that is large enough to represent diffuse, dipole-bound states.

In recognition of the need for a diffuse basis set, we first solved for the pseudo-orbital using the atom-centered 6-31++G basis set, which includes diffuse functions at each atomic site. The pseudo-orbital in this basis was nodeless, as required by our formalism, but the eigenenergy of the pseudo-orbital was highly unbound, with an energy of +1.45 eV. Repeating the calculation with larger and increasingly diffuse atom-centered basis sets resulted only in minor decreases in the pseudo-orbital energy. Thus, even though we expected the pseudo-orbital to be weakly bound, to better understand precisely what was causing the pseudo-orbital energy to be unbound, we went ahead and used the atom-centered 6-31++G basis to calculate the effective pseudopotential via Eq. (7). As illustrated by the dashed curves in Fig. 2, the effective potential calculated using this basis is dominated by an unphysical quadratic divergence that starts $\sim 10a_0$ from the THF center of mass. This quadratic divergence is an artifact of choosing a spatially localized, atomic-centered basis set, which artificially confines the excess electron density to a region near the THF molecular frame, resulting in an unrealisticly repulsive eigenenergy. Mathematically, this divergence arises because an asymptotically decaying Gaussian wave function is associated with a harmonic potential. To remove this unphysical divergence of the pseudopotential, we augmented our atomic-centered 6-31++G basis with an additional $8^3=512$ *s*-type Gaussian primitives with decay constant of $0.000\,474a_0^{-2}$ that were evenly distributed on a cubic grid with sides of length $150a_0$; we refer to this augmented basis as 6-31++G(AUG). We explored a number of grid sizes, spacings, and density of augmented functions before finalizing our basis set choice; we settled on our final choice of 512 augmented functions on a grid with side of length of $150a_0$ because, as Fig. 2 shows, the calculated potential (solid curves) matched well to the expected long-range dipole potential, $U_{\text{dipole}}=\mu/r^3$ (dotted curves), where μ is the calculated dipole moment of THF.

A careful inspection of Fig. 2(b), however, shows that the correspondence between the effective potential calculated with the 6-31++G(AUG) basis and the asymptotically exact long-range dipole potential is not perfect. This is because even an augmented Gaussian basis set is simply incapable of reproducing the exact asymptotic limit. A pseudo-orbital with an asymptotic Gaussian decay always produces a pseudopotential that is asymptotically quadratic. Thus, we found it necessary to taper the numerical pseudopotential, U_{eff}, into the correct asymptotic form. In order to guarantee a smooth transition, we employed an ellipsoidal tapering function,

$$U_{\text{total}} = U_{\text{eff}}(1 - t(\mathbf{r})) + U_{\text{dipole}}t(\mathbf{r}), \tag{9}$$

where

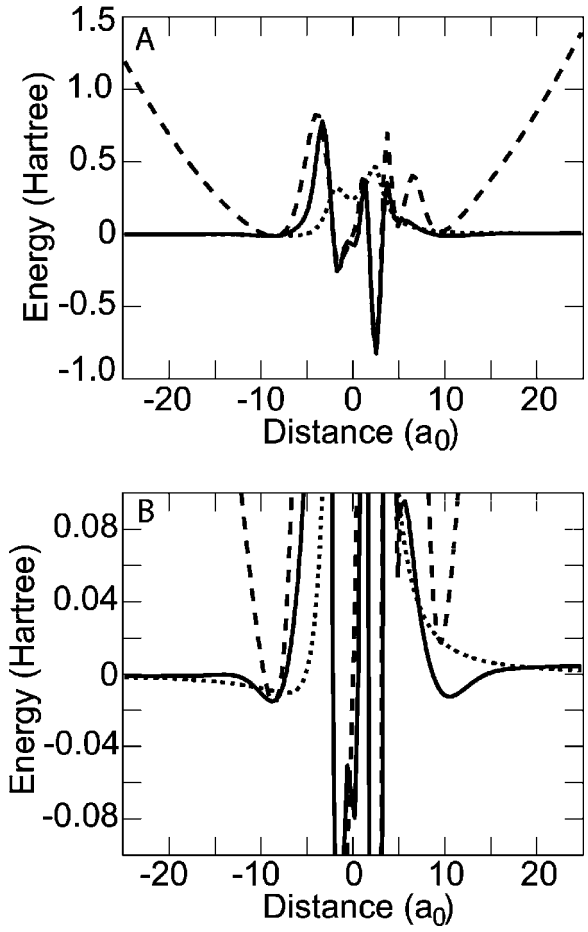

FIG. 2. Correcting the divergence of THF-e^- effective potential, Eq. (7), at large distances due to the choice of a Gaussian basis set. Panel A shows one-dimensional (1D) cuts of the effective potential along the principal symmetry axis of THF calculated using different basis sets. The dashed curve is the effective potential generated with the atom-centered 6-31++G basis set, and the solid curve is the effective potential calculated with a 6-31++G(AUG) basis, which includes off-molecule diffuse basis functions as described in the text. The exact asymptotic long-range potential, based on the Mulliken charges, is shown as the dotted curve. Use of a nonaugmented basis set produces an effective potential whose asymptotic behavior is entirely unphysical (see text). Panel B shows the same data as panel A but on an expanded scale to facilitate comparison between the different potentials.

$$t(\mathbf{r}) = \frac{1}{e^{-10(f(\mathbf{r})-1)}+1}, \tag{10}$$

and

$$f(\mathbf{r}) = f(x,y,z) = \frac{x^2}{x_0^2} + \frac{y^2}{y_0^2} + \frac{(z-1.0)^2}{z_0^2}, \tag{11}$$

and the constants $(x_0, y_0, z_0) = (12.5a_0, 12.0a_0, 16.0a_0)$ were selected to coincide with points of nearest crossings between the short-range 6-31++G(AUG) potential and the long-range dipole potential. Here, the origin of the coordinates is at the center of mass of the THF molecule. It is worth noting that had we elected to taper the nonaugmented basis set in this fashion, we would have produced a pseudopotential that is incorrect in the core region of the molecule [cf. Fig. 2(b)]. Even though the nonaugmented basis set describes the core orbitals perfectly well, the fact that it produces the wrong asymptotic behavior for the pseudo-orbital starting so close to the molecule leads to a calculated pseudopotential that is incorrect in the region of the core.

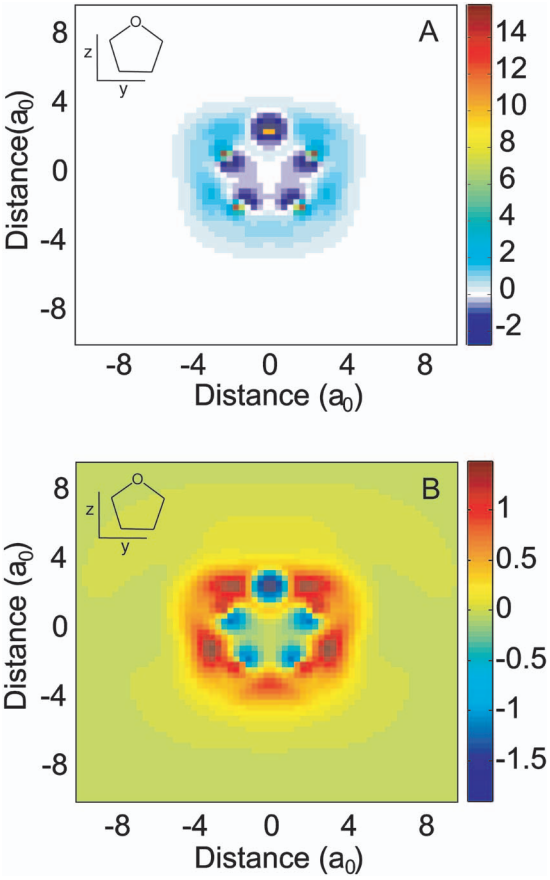

FIG. 3. (Color) 2D cuts of the exact effective e-THF potential parallel to the molecular plane. The magnitude of the potential in each panel, given by the color scale, is in hartrees and the spatial axes have units of bohr radii. The schematic THF molecule drawn in the top left corner of each panel illustrates the perspective of the cut as well as the Cartesian axis labels used for the fit described in Table I. The cut in Panel A is $0.16a_0$ above the molecular plane; the cut in panel B is $0.48a_0$ above the molecular plane. Note that the color scale is not the same in the two panels, and that the magnitude of the potential decays quickly with increasing distance from the molecular plane.

D. The exact THF-e^- effective potential

With our choice of the 6-31++G(AUG) basis and the asymptotic tapering procedure described in Sec. II C, we calculated the effective potential of an excess electron interacting with a THF molecule on an evenly spaced 64^3 grid spanning $-10a_0$ to $10a_0$ on a side. Representative two-dimensional (2D) cuts through the full three-dimensional (3D) effective potential are shown in Figs. 3 and 4; the origin in both of these figures is set at the center of mass of the THF molecule, and the orientation of the THF backbone for each cut is shown in the top left corner of each panel.

Figure 3 shows two slices of the effective potential in planes parallel to the molecular backbone; panel A shows a cut $0.16a_0$ above the THF plane and panel B shows a cut $0.48a_0$ above the molecular plane. The cut directly through the molecular plane is not shown since the potential is completely dominated by features centered at the atom sites that act to obscure most of the other details of the potential. The first thing to note is that the shape of effective potential is

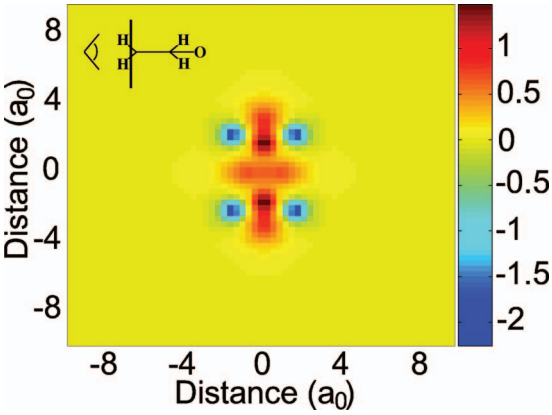

FIG. 4. (Color) 2D cut of the exact effective e-THF potential perpendicular to the molecular plane. As with Fig. 3, the color scale gives the potential energy in hartrees and the distance units are in bohr radii. The viewing perspective of this cut is indicated in the top left corner, where the vertical bar near the β hydrogens represents the plane in which the potential is shown. The strong effect of the hydrogen atoms is clearly visible as the four attractive centers above and below the THF plane.

quite complex. It is evident in both panels of Fig. 3 that there are several features of the effective potential that are centered on neither the atomic sites nor the molecular bonds. The presence of such features highlights the importance of using the exact pseudopotential formalism instead of attempting to model the core MO electronic structure. Model potentials based on atom-site and midpoint contributions (which both we[2] and others[20] have used in previous work) do not necessarily incorporate the appropriate physics. The next feature of the effective potential worth noting upon inspection of Fig. 3 is the strongly repulsive spikes near each atomic center. The presence of these repulsive features makes good physical sense. The purpose of the pseudopotential is to force orthogonality between the excess electron and the electrons in the core MOs, including the deeply buried atomic core orbitals on each atom in the molecule. Thus, the strong repulsive feature seen at the oxygen site in Fig. 3(a) prevents the excess electron from collapsing onto the lowest MO of the THF molecule, which is the oxygen 1s atomic orbital. The two strong features located to either side of the oxygen site provide a similar repulsion that is likely due to the enforced orthogonality with the electrons in the oxygen lone pairs. The fact that these repulsive spikes originate primarily from repulsion from the atomic core orbitals is verified in Fig. 3(b), which shows that by $0.48a_0$ above the molecular plane, there is no longer any strong repulsion from the oxygen atomic site. Indeed, a comparison of the two panels shows that the effective potential around the oxygen site is a compact repulsive ball centered in a larger attractive shell. The two panels also make it apparent that the effective potential near each atomic carbon site has a p-like feature with the repulsive lobe pointing away from the molecule.

Figure 4 shows the calculated effective potential from another perspective, this time in a cut perpendicular to the molecular plane near the β-hydrogen sites; the backbone orientation is shown in the top left corner of the figure. A comparison of Figs. 3 and 4 shows that the spatial extent of the various features in the effective potential is not the same in the molecular plane as above and below the plane. More importantly, Fig. 4 shows that in addition to the carbon and oxygen atoms, the hydrogen atoms also produce well-defined features in the effective potential. The H-atom features are attractive for the excess electron, which is perhaps not surprising given that the electronic structure of the planar THF molecule has positively-charged hydrogens (the Mulliken charge for the H atoms from the Gaussian calculation is close to $+0.1$). Since repulsive terms in the effective potential arise from orthogonality constraints with core MOs, in regions where there is little core electron density, the attractive nuclear terms will dominate. The fact that the hydrogen atoms make a significant contribution to the total effective potential indicates that the use of a united-atom approach will sacrifice accuracy; there is clearly a need to explicitly include the hydrogen sites to correctly describe the interaction. Given the nature of the carbon-hydrogen chemical bond, it would seem that the pseudopotential for an excess electron interacting with virtually any hydrocarbon should also require explicit inclusion of the hydrogen atom sites.

III. FIT OF EFFECTIVE POTENTIAL FOR USE IN MOLECULAR SIMULATION

Our principal interest in calculating the effective potential of an excess electron interacting with THF is for use in mixed quantum/classical molecular dynamics simulations of solvated electrons and sodium anions in liquid THF. The previous section presented the details of how we calculated the exact effective potential. Given the relatively large number of basis functions and the need to taper the long-range dipole potential, on-the-fly calculation of the exact effective potential, using Eq. (7), is simply too tedious to be practical for molecular simulation. Instead, we need an easily evaluated analytic function that closely approximates the effective potential for use in molecular dynamics calculations. The exact effective potential, which includes contributions from the five backbone atoms, the eight hydrogen atoms, and a few sites that are not associated with any of the atoms or bond midpoints, is sufficiently complex that a fairly large parameter space is required for an accurate fit. Thus, we chose to fit our effective potential to a function with a large number of free parameters even though such a complex nonlinear fit can be somewhat computationally demanding. However, the fit only has to be calculated once, and as long as the total number of parameters is similar to that used in simpler models, the increase in accuracy compensates for any additional cost to the actual molecular simulations.

We performed the fit using the unconstrained nonlinear fitting routine *lsqcurvefit.m* in the MATLAB 7 Release 14 statistics toolbox with the numerical pseudopotential evaluated on a 64^3 grid of side length of $20a_0$ centered on the THF molecule. The 55-parameter function to which we chose to fit our effective THF-e^- potential, along with a summary of the best-fit parameters, is presented in Table I. Our fit function is comprised of 18 different sites, and these sites fall into two different classes, atom-centered sites and sites not located on the molecular framework. If a function is centered on an atom site, we label the position vector by the atomic symbol followed by a unique atom descriptor. For example,

TABLE I. Functional form and parameters of the fit to the exact e^--THF Effective potential. The 55-parameter fit has functional contributions centered on 18 different sites. Parameters with a plus/minus sign are to be read as follows: the top sign corresponds to sites situated to the right of the oxygen atom, as depicted in Fig. 1, and the bottom sign to sites on the left. All parameters are given in a.u.

$$U_{\mathrm{fit}}(\mathbf{r}) = \begin{cases} U_o + U_{c\alpha 1} + U_{c\alpha 2} + U_{c\beta 1} + U_{c\beta 2} + U_{h\alpha 1} + U_{h\alpha 2} + U_{h\alpha 3} + U_{h\alpha 4} \\ + U_{h\beta 1} + U_{h\beta 2} + U_{h\beta 3} + U_{h\beta 4} + U_{ao1} + U_{ao2} + U_{ac1} + U_{ac2} + U_{aa} \end{cases}$$

$$U_o(\mathbf{r}-\mathbf{r}_o) = \begin{array}{l} (o_1(x-x_o)^4 - o_2(y-y_o)^4 + o_3(z-z_o)^4 - o_4) \\ \times \exp(-[o_5(x-x_o)^2 + o_6((y-y_o)^2 + (z-z_o)^2)]) + o_7 \dfrac{\exp[-o_8(\mathbf{r}-\mathbf{r}_o)^2]}{|\mathbf{r}-\mathbf{r}_o|} \end{array}$$

$o_1 = 1.2725$	$o_2 = 1.533$	$o_3 = 0.8261$	$o_4 = 5.7327$
$o_5 = 1.099$	$o_6 = 1.1081$	$o_7 = 30.6889$	$o_8 = 47.9705$

$$U_{c\alpha}(\mathbf{r}-\mathbf{r}_{c\alpha}) = \begin{array}{l} c_1^\alpha[(y-y_{c\alpha}) + c_2^\alpha(z-z_{c\alpha})] \times \exp(-[c_3^\alpha(x-x_{c\alpha})^2 + c_4^\alpha((y-y_{c\alpha})^2 + (z-z_{c\alpha})^2)]) \\ - c_5^\alpha \dfrac{1}{|\mathbf{r}-\mathbf{r}_{c\alpha}|} + c_6^\alpha \exp[-c_7^\alpha(\mathbf{r}-\mathbf{r}_{c_\alpha})^4] \end{array}$$

$c_1^\alpha = \pm 37.6869$	$c_2^\alpha = \pm 1.6332$	$c_3^\alpha = 9.4354$	$c_4^\alpha = 8.7066$
$c_5^\alpha = 0.6278$	$c_6^\alpha = 8.3378$	$c_7^\alpha = 31.8109$	

$$U_{c\beta}(\mathbf{r}-\mathbf{r}_{c\beta}) = \begin{array}{l} c_1^\beta[(y-y_{c\beta}) + c_2^\beta(z-z_{c\beta})] \times \exp[-(c_3^\beta(x-x_{c\beta})^2 - c_4^\beta((y-y_{c\beta})^2 + (z-z_{c\beta})^2))] \\ + c_5^\beta \dfrac{1}{|\mathbf{r}-\mathbf{r}_{c\beta}|} + c_6^\beta \exp[-c_7^\beta(\mathbf{r}-\mathbf{r}_{c\beta})^4] \end{array}$$

$c_1^\beta = \pm 51.8110$	$c_2^\beta = \mp 0.7854$	$c_3^\beta = 8.7918$	$c_4^\beta = 8.1685$
$c_5^\beta = 0.08500$	$c_6^\beta = 6.8727$	$c_7^\beta = 35.6946$	

$$U_{h\alpha}(\mathbf{r}-\mathbf{r}_{h\alpha}) = -h_1^\alpha \frac{\exp[-h_2^\alpha(\mathbf{r}-\mathbf{r}_{h\alpha})^2]}{|\mathbf{r}-\mathbf{r}_{h\alpha}|} + h_3^\alpha \exp[-h_4^\alpha(\mathbf{r}-\mathbf{r}_{h\alpha})^2]$$

$h_1^\alpha = 0.8962$	$h_2^\alpha = 1.4133$	$h_3^\alpha = 0.1097$	$h_4^\alpha = 0.02756$

$$U_{h\beta}(\mathbf{r}-\mathbf{r}_{h\beta}) = -h_1^\beta \frac{\exp[-h_2^\beta(\mathbf{r}-\mathbf{r}_{h\beta})^2]}{|\mathbf{r}-\mathbf{r}_{h\beta}|} + h_3^\beta \exp[+h_4^\beta(\mathbf{r}-\mathbf{r}_{h\beta})^2]$$

$h_1^\beta = 0.8724$	$h_2^\beta = 1.2483$	$h_3^\beta = 0.0171$	$h_4^\beta = 9.9500 \times 10^{-5}$

$$U_{ao}(\mathbf{r}-\mathbf{r}_{ao}) = a_1^o \exp[-(a_2^o(x-x_{ao})^2 + a_3^o(y-y_{ao})^2 + a_4^o(z-z_{ao})^2)]$$

$a_1^o = 2.0060$	$a_2^o = 0.6310$	$a_3^o = 0.1956$	$a_4^o = 0.7790$
$x_{ao} = 0.0000$	$y_{ao} = \pm 1.3379$	$z_{ao} = 2.3062$	

$$U_{ac}(\mathbf{r}-\mathbf{r}_{ac}) = a_1^c \exp[-(a_2^c(x-x_{ac})^2 + a_3^c(y-y_{ac})^2 + a_4^c(z-z_{ac})^2)]$$

$a_1^c = 1.4982$	$a_2^c = 0.5106$	$a_3^c = 0.9371$	$a_4^c = 0.2384$
$x_{ac} = 0.0000$	$y_{ac} = \pm 3.1504$	$z_{ac} = -0.7839$	

$$U_{aa}(\mathbf{r}-\mathbf{r}_{aa}) = \begin{array}{l} a_1^a \exp[-(a_2^a(x-x_{aa})^2 + a_3^a(y-y_{aa})^2 + a_4^a(z-z_{aa})^2)] \\ - a_5^a \exp[-(a_6^a(x-x_{aa})^2 + a_7^a(y-y_{aa})^2 + a_8^a(z-z_{aa})^2)] \end{array}$$

$a_1^a = 12.0383$	$a_2^a = 0.8467$	$a_3^a = 0.3176$	$a_4^a = 0.4038$
$a_5^a = 11.2602$	$a_6^a = 0.8985$	$a_7^a = 0.3376$	$a_8^a = 0.3724$
$x_{aa} = 0.0000$	$y_{aa} = 0.0000$	$z_{aa} = -3.41519$	

$\mathbf{r}_{c\alpha 2}$ refers to the position of one of the α carbons. The fit parameters associated with each atom site are labeled similarly, for example, c_1^{α} is the first parameter associated with a fit function centered on one of the α-carbon atoms. For fit functions that are not associated with atomic sites on the molecular frame, we denote the position vectors as $\mathbf{r}_{a\{\text{site}\}}$ where {site} is a label to indicate its location. We have chosen the following notation for the off-molecule sites: *ao*(1 and 2) refer to the two features near the oxygen atom, *ac*(1 and 2) refer to the features near the β-carbon atoms, and *aa* refers to the aft feature on the molecular axis (cf. Figs. 3 and 4).

One of our chief motivations in our choice of fit function was to try to keep physical insight into the origins of the effective potential. For example, we expect the effective potential associated with each of the atom sites to have some local r^{-1} character since the core electrons do not perfectly shield the nuclei from the excess electron; indeed, the damped r^{-1} form is the dominant characteristic of the effective potential near the H atoms. In addition, the rapidly decaying repulsive spike on the oxygen atom visible in Fig. 3(a) also fits well to an r^{-1} form; as discussed above, surrounding this spike is an attractive well that we found was adequately fit with a fourth-order polynomial in each direction. The angled *p*-like features centered on the carbon sites seen in Fig. 3(b) fit well to *p*-like cartesian Gaussians. One of the key features of the effective potential that made it so difficult to fit is the fact that the general decay of the potential is different in the molecular plane versus normal to it; thus, the biggest improvements were achieved by allowing each the fit functions to have different decay constants in different directions. This anisotropy is particularly apparent in the features located to either side of the oxygen atom, which fit quite well to Gaussians but with decay constants that differ by a factor of ~3 in different directions. The other off-atom sites were similarly well treated with anisotropic Gaussians.

Figure 5(a) shows the fit, with the parameters quoted in Table I, for a cut parallel to the THF molecular plane but $0.16a_0$ above it; this is the same cut for which the exact effective potential is shown in Fig. 3(a). Figure 5(b) plots the difference between the fit and the exact potential in this plane. Although residual features are clearly visible in Fig. 5(b), the amplitude of the difference is quite small relative to the size of the features in the exact potential. The only region where we are somewhat unsatisfied with the quality of the fit is around the carbon atoms, but we found it difficult to improve the fit without the addition of many more functional parameters. In EPAPS Document No. E-JCPA6-125-502628, we present the values of the exact effective potential calculated from $-10a_0$ to $10a_0$ on a 64^3 evenly spaced cubic grid for any researchers who wish to perform alternate fits or who wish to investigate cuts of the exact potential that we have not shown in this paper.[31]

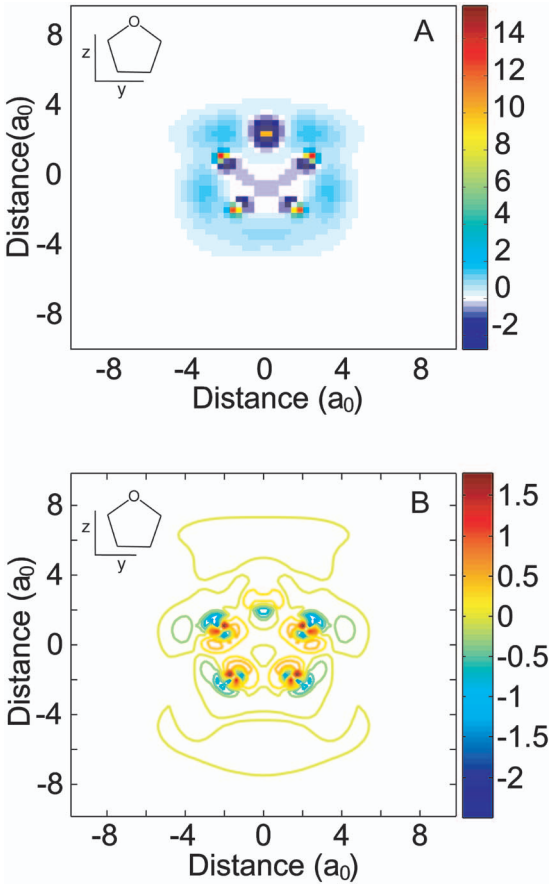

FIG. 5. (Color) Fit to the exact e^--THF effective potential. Panel A shows a 2D cut of the 55-parameter fit (see Table I and text) parallel to the THF molecular plane and $0.16a_0$ above it; this is the same cut for which the exact effective potential is shown in Fig. 3(a). Panel B shows the residuals of the fit, i.e., the difference between Figs. 5(a) and 3(a).

IV. CONCLUSIONS

In this paper, we have presented a computational methodology for calculating the exact effective potential for molecular systems via the solution to Eqs. (7) and (8). We have illustrated this methodology by calculating the effective potential for an excess electron interacting with a THF molecule, which as far as we are aware is the most complex system for which an exact pseudopotential has been calculated. We also found that the use of an augmented basis set is critical to capturing the correct asymptotic behavior of the LUMO and thus the pseudopotential. Without the use of off-atom, long-range diffuse basis functions, the calculated effective potential contains significant errors, even in the region of the molecular core. In addition, to use our calculated e^--THF effective potential in mixed quantum/classical simulations, we also presented a physically motivated fit to the exact potential. As we pointed out in the preceding paper, for some applications it may be necessary to smooth the pseudopotential. We will demonstrate in a subsequent publication how to smooth the pseudopotential by first smoothing the pseudo-orbital.[32] Finally, we note that with our computationally efficient formalism, the calculations presented here lie on the low end of computational feasibility; the iterative solution of Eq. (8) for the e^--THF effective potential presented above took less than 3 s on a somewhat modest single processor. This makes it clear that our formalism could be used to calculate effective potentials for much larger molecules. Since the potential energy evaluation of the pseudo-orbital is

entirely excluded from such calculations in our formalism, the only limit to the size of the system for which an exact pseudopotential can be calculated is the ability to obtain the original core and valence electron wave functions for the system of interest.

ACKNOWLEDGMENTS

This work was supported by the National Science Foundation under Grant No. CHE-0240776. One of the authors-(B.J.S.) is a Camille Dreyfus Teacher-Scholar. The authors gratefully acknowledge UCLA Academic Technology Services for the use of its Hoffman Cluster and other computational resources.

[1] W. E. Pickett, Comput. Phys. Rep. **9**, 115 (1989).
[2] M. J. Bedard-Hearr, R. E. Larsen, and B. J. Schwartz, J. Chem. Phys. **122**, 134506 (2005).
[3] C. J. Smallwood, W. B. Bosma, R. E. Larsen, and B. J. Schwartz, J. Chem. Phys. **119**, 11263 (2003).
[4] K. F. Wong and P. J. Rossky, J. Phys. Chem. A **105**, 2546 (2001).
[5] W. S. Sheu and P. J. Rossky, J. Phys. Chem. **100**, 1295 (1996).
[6] D. F. Coker and B. J. Berne, *Quantum Calculations of Excess Electrons in Disordered Media, Excess Electrons in Dielectric Media* (CRC, Boca Raton, FL, 1991).
[7] L. Szasz, *Pseudopotential Theory of Atoms and Molecules* (Wiley-Interscience, New York, 1985).
[8] J. C. Phillips and L. Kleinman, Phys. Rev. **116**, 287 (1959).
[9] J. Schnitker and P. J. Rossky, J. Chem. Phys. **86**, 3462 (1987).
[10] I. Abarenkov and V. Heine, Philos. Mag. **12**, 529 (1965).
[11] R. W. Shaw, Phys. Rev. **174**, 769 (1968).
[12] C. J. Smallwood, R. E. Larsen, W. J. Glover, and B. J. Schwartz J. Chem. Phys. **175** 074102 (2006), preceding paper.
[13] I. B. Martini, E. R. Barthel, and B. J. Schwartz, J. Chem. Phys. **113**, 11245 (2000).
[14] I. B. Martini and B. J. Schwartz, Chem. Phys. Lett. **360**, 22 (2002).
[15] E. R. Barthel, I. B. Martini, and B. J. Schwartz, J. Chem. Phys. **112**, 9433 (2000).
[16] E. R. Barthel, I. B. Martini, and B. J. Schwartz, J. Phys. Chem. B **105**, 12230 (2001).
[17] E. R. Barthel and B. J. Schwartz, Chem. Phys. Lett. **375**, 435 (2003).
[18] I. B. Martini, E. R. Barthel, and B. J. Schwartz, Pure Appl. Chem. **76**, 1809 (2004).
[19] I. B. Martini, E. R. Barthel, and B. J. Schwartz, J. Am. Chem. Soc. **124**, 7622 (2002).
[20] Z. H. Liu and B. J. Berne, J. Chem. Phys. **99**, 9054 (1993).
[21] M. H. Cohen and V. Heine, Phys. Rev. **122**, 1821 (1961).
[22] L. Turi, M. P. Gaigeot, N. Levy, and D. Borgis, J. Chem. Phys. **114**, 7805 (2001).
[23] L. Turi and D. Borgis, J. Chem. Phys. **117**, 6186 (2002).
[24] A. Szabo and N. Ostlund, *Modern Quantum Chemistry* (Dover, New York, 1996).
[25] M. A. Morrison and L. A. Collins, Phys. Rev. A **17**, 918 (1978).
[26] M. J. Frisch, G. W. Trucks, H. B. Schlegel, *et al.*, Gaussian, Inc., Pittsburgh, PA, 1998.
[27] J. Chandrasekar and W. L. Jorgensen, J. Chem. Phys. **77**, 5073 (1982).
[28] E. Anderson, Z. Bai, C. Bischof, S. Blackford, J. Demmel, J. Dongarra, J. Du Croz, A. Greenbaum, S. Hammarling, A. McKenney, and D. Sorenson, *LAPACK User's Guide*, 3rd edition (Society for Industrial and Applied Mathematics, Philadelphis, 1999.
[29] *Handbook of Chemistry and Physics*, 81st ed., edited by D. R. Lide (CRC, Boca Raton, FL, 2000).
[30] K. D. Jordan and F. Wang, Annu. Rev. Phys. Chem. **54**, 367 (2003).
[31] See EPAPS Document No. E-JCPSA6-125-502628 which gives the numerically calculated effective potential on an evenly spaced 64^3 cubic grid running from $-10a_0$ to $10a_0$ in each direction. This document can be reached via a direct link in the online article's HTML reference section or via the EPAPS homepage (http://www.aip.org/pubservs/epaps.html).
[32] C. N. Mejia, R. E. Larsen, and B. J. Schwartz (unpublished).